JOURNAL OF AIRCRAFT
Vol. 38, No. 3, May–June 2001

Dynamic Stall Control by Periodic Excitation, Part 1: NACA 0015 Parametric Study

D. Greenblatt* and I. Wygnanski†
Tel Aviv University, 69978 Ramat Aviv, Israel

A parametric study was undertaken to investigate the effect of periodic excitation (with zero net mass flux) on a NACA 0015 airfoil undergoing pitch oscillations at rotorcraft reduced frequencies under incompressible conditions. The primary objective of the study was to maximize airfoil performance while limiting moment excursions to typical prestalled conditions. The incidence angle excursions were limited to ± 5 deg, and a wide range of reduced excitation frequencies and amplitudes were considered for $0.3 \times 10^6 \leq Re \leq 0.9 \times 10^6$ with various flap deflections and excitation locations. Significant increases in maximum lift and reductions in drag were attained while containing the moment excursions. Oscillatory excitation was found to be far superior to steady blowing, which was even detrimental under certain conditions, and flap-shoulder excitation was found to be superior to leading-edge excitation.

Nomenclature

C_D	=	drag coefficient, D/cq
C_{Dp}	=	form-drag coefficient, Dp/cq
C_L	=	lift coefficient, L/cq
$C_{L,\text{exc}}$	=	lift coefficient excursion
$C_{L,\max}$	=	maximum lift coefficient
C_M	=	pitching moment coefficient, M/c^2q
C_P	=	pressure coefficient, $(p - p_\infty)/q$
C_μ	=	steady momentum coefficient, J/cq; rms momentum coefficient, $\langle J \rangle/cq$
c	=	airfoil chord
E	=	moment excursion, $C_{M,\max} - C_{M,\min}$
F^+	=	reduced excitation frequency, $f_e X_{te}/U_\infty$
f_a	=	airfoil oscillation frequency
f_e	=	excitation frequency
h	=	slot width
J	=	steady jet momentum, $\rho U_j^2 h$
$\langle J \rangle$	=	rms jet momentum, $\rho \langle u_J \rangle^2 h$
k	=	reduced airfoil frequency, $\pi f_a c/U_\infty$
M	=	Mach number
p	=	local pressure
q	=	freestream dynamic pressure, $\rho U_\infty^2/2$
Re	=	chord Reynolds number, $\rho U_\infty c/\mu$
u, U	=	oscillatory, mean velocity
X_{te}	=	distance from slot location to trailing edge
x/c	=	normalized chordwise distance
α	=	instantaneous incidence angle
$\bar{\alpha}$	=	mean incidence angle
δ_f	=	flap deflection angle
μ	=	air dynamic viscosity
ρ	=	air density
$\langle\ \rangle$	=	rms quantity

Subscripts

A	=	allowable excursions
exc	=	excursion of aerodynamic coefficient
mean	=	time mean of aerodynamic coefficient
s	=	static stall angle
∞	=	freestream conditions

Received 11 December 1998; revision received 6 September 1999; accepted for publication 8 September 2000.

*Postdoctoral Fellow, Department of Fluid Mechanics and Heat Transfer, Faculty of Engineering. Member AIAA.

†Lazarus Professor of Aerodynamics, Department of Fluid Mechanics and Heat Transfer, Faculty of Engineering; currently Professor of Aerospace Engineering, Department of Aerospace and Mechanical Engineering, P.O. Box 210119, 1130 N. Mountain, RM N614, University of Arizona, Tucson, Arizona 85721-00119. Fellow AIAA.

I. Introduction

DYNAMIC stall limits the maximum cruising speed of modern helicopters due the excessive and damaging loads that it generates on the rotors.[1] The dominant feature characterizing dynamic stall is a strong vortex, which begins near the leading edge, enlarges, and then travels downstream. This so-called dynamic stall vortex (DSV) brings about abrupt variations in lift as well as sharp increases in drag with strong concomitant pitching moments. Dynamic stall may be classified as light (where the viscous-dominated zone is of the order of the airfoil thickness) or deep (where the incidence angle is well in excess of the static stall angle, resulting in a totally separated region that is commensurate with the chord dimensions).[2]

As a consequence of dynamic stall's negative impact, much basic research has focused on controlling (managing) or eliminating the phenomenon. Boundary-layer control[3] has been employed for rotorcraft applications and includes methods such as blowing,[1,4] suction,[5,6] and pulsed blowing,[7,8] as well as control of boundary-layer transition.[9–11] Modifications to airfoil geometry such as leading-edge slats,[12–14] leading-edge droop,[14] rotation of the leading-edge,[15] as well as dynamically deforming geometries[16] have been investigated. In all cases, these changes are geared specifically to the leading-edge region where the dynamic-stall vortex originates. To date, the various attempts to contain the DSV have been confined to experimental configurations and numerical studies and have not, as yet, found application. The need to control dynamic stall, however, has recently received renewed impetus as the next generation of military helicopters demand dramatic increases in performance envelopes to meet projected requirements.[12,17] Because the current rotor sections fall short of these capabilities,[12] alternative viable methods must be investigated if the projected performance levels are to be attained.

It has been conclusively shown, in recent years, that periodic excitation is far more effective in delaying static stall than traditional steady blowing. This has been illustrated for a generic-flap,[18–21] various airfoils,[22,23] and a swept-back wing,[24] as well as compressible[25] and high Reynolds numbers flows.[26] Moreover, the method has been demonstrated as being capable of controlling dynamic stall and significantly improving dynamic airfoil performance.[27–29] Specifically, significant increases in maximum lift and reductions in form drag were attained while containing moment excursions.[28] Based on these provisional findings, a detailed parametric study was undertaken and a summary of important results is presented in this paper. Note that the companion paper[30] places emphasis on the flow mechanisms associated with both dynamic stall as well as the nature of its control.

II. Experimental Setup

Experiments were carried out on a 365-mm chord NACA0015 airfoil, incorporating 36 pressure taps, a $0.25c$ trailing-edge flap, and two surface-tangential (leading-edge and flap-shoulder) two-dimensional slots.[28,31] The airfoil was installed in the test section of a closed-loop 610 (span) × 1524 mm low-speed wind tunnel[23] and equipped with $0.1c$ roughness strips on both surfaces. Total drag was measured by means of a stepper-motor controlled wake rake. All dynamic pressure measurements were made with a PS4000 multichannel array of pressure transducers (AA Lab Systems). A pitch drive system, used by Piziali,[32] generated a sinusoidal pitching motion about the one-quarter chord position, and a shaft-mounted encoder signal was used to ascertain the instantaneous incidence angle. Encoder and pressure data were simultaneously transferred, via DMA, to a personal computer. Zero net mass-flux excitation was achieved by means of a rotating valve and a small centrifugal blower connected to the airfoil plenum chamber.[23] Hot-wire calibration of the resulting jets produced at the slot exits was performed within the top-hat region, for the frequency range $0 \le f_e \le 400$, at 50-mm intervals along the span of the airfoil.[31] This calibration was used to determine both the steady momentum coefficient, $C_\mu = J/cq$, and the rms momentum coefficient, $C_\mu = \langle J \rangle / cq$, for steady, $f_e = 0$, or oscillatory, $f_e > 0$, jets, respectively. Note that, because $f_e \gg f_a$, a phase relation between excitation and pitching oscillations was considered unnecessary and, therefore, not enforced.[30]

III. Strategy and Objectives

On the basis of preliminary data,[27,28] a detailed parametric study was undertaken, under incompressible conditions where the following method was adopted.

1) The static-stall angle α_s was determined for the airfoil at a particular Reynolds number (Fig. 1).

2) The mean airfoil oscillation angle was set at $\alpha_s - 5$ deg and was oscillated at a frequency corresponding to typical dimensionless rotor frequencies, $k \equiv \pi f_a c / U_\infty$, at α excursions of ±5 deg.

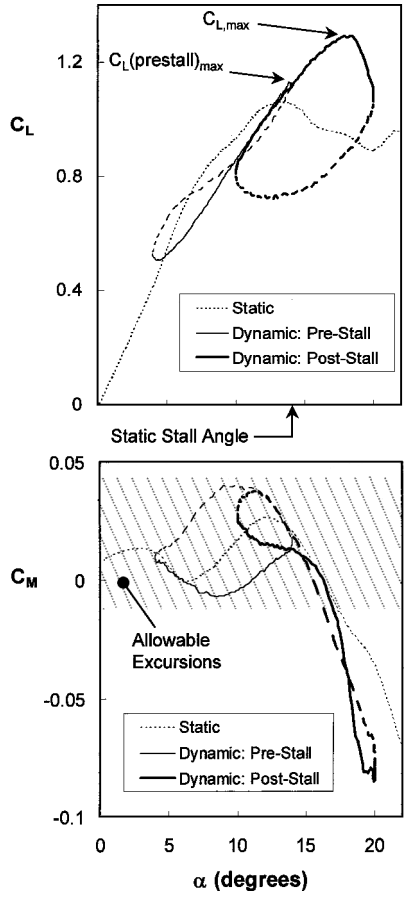

Fig. 1 Basis for the parametric study.

3) The prestall moment-coefficient excursions $E_{\rm ps} = C_{M,\max} - C_{M,\min}$ were recorded, and an arbitrary fractional tolerance ε was added to the excursions, thus defining the maximum allowable excursions $E_A = (1 + \varepsilon) E_{\rm ps}$.

4) The mean incidence angle, with the same (±5 deg) excursions was then increased such that the airfoil entered the poststall regime.

5) When excitation at different frequencies and amplitudes was employed and compared with steady blowing, an attempt was made to attain the highest possible $C_{L,\max}$ for a particular cycle while maintaining the condition $E \le E_A$. No attempt was made to vary the excitation amplitude, that is, C_μ within the airfoil oscillation cycle.

In addition to illustrating the strategy, Fig. 1 shows the effect of increasing the mean incidence angle by 6 deg without excitation or blowing. Clearly, a higher $C_{L,\max}$ is attained, but the moment excursions are unacceptably large. The strategy just described seeks to maintain or increase $C_{L,\max}$ while bounding the moment excursions to within acceptable values (thatched region in Fig. 1). Although moment stall commenced at $\alpha = 13$ deg, the static-stall angle was fixed at the $C_{L,\max}$ location ($\alpha = 14$ deg).

Note that currently no formal theory exists for predicting separation delay by oscillatory addition of momentum, although computational fluid dynamics has been successful in predicting some gross characteristics.[33] The current problem is further complicated by the combination of pitching, f_a, and excitation, f_e, frequencies. The companion paper,[30] however, emphasizes the general principle of time scale disparity (alternatively $f_e \gg f_a$) and shows that the net effect of excitation is not significantly altered by f_a. Using this as a basis, and notwithstanding qualitative differences between the airfoil[22,34] and the generic flap,[21] the observations reported here are assessed on the basis of their consistency with the generic-flap parametric study.[20,21]

IV. Discussion of Results

Table 1 contains a list of the parameters considered in this study. Most of the data were acquired at $Re = 0.3 \times 10^6$ because this allowed a greater range of F^+ and C_μ, thus ensuring greater flexibility of the parametric study. The marginal effect of Reynolds number on separation control by excitation was established for static airfoils[25] and was also demonstrated for dynamic stall.[31,35] The rationale behind maintaining incidence excursions constant ($\Delta\alpha = \pm 5$ deg) was based in the principle of matched pitch rate,[1,36] where larger excursions can be simulated by larger airfoil oscillation rates, and was confirmed in the current context.[31]

In certain cases where a large amount of data were compared, the following aerodynamic indicators were selected: $C_{L,\max}$ (or excursions $C_{L,\rm exc} \equiv C_{L,\max} - C_{L,\min}$), moment excursions $C_{M,\max} - C_{M,\min}$, and time mean C_{Dp} (form drag) or C_D (total drag). These are clearly not the only quantities of importance, but in accordance with the main objective of this parametric study, they served as the best indicators of overall airfoil performance. The number of loops required to achieve statistically independent data varied between 5 and 50, depending on the prevailing flow conditions.[31,37] It was ascertained for all flap deflection cases considered that $E_{\rm ps} \approx 0.05$. Thus, with $\varepsilon = 0.2$, the maximum allowable moment excursion limit was $E_A = 0.06$, although the use of smaller or larger values did not

Table 1 Range of investigated parameters

Parameter	Range
$Re \times 10^6$	0.3–0.9
k	0.05–0.3
Ma	≤0.12
$\bar{\alpha}$, deg	5–20
$\Delta\alpha$, deg	±5
C_μ,%	~0.01–5
F^+	~0.3–5
δ_f, deg	−10–20
Location	Leading-edge and flap shoulder

in any way affect the major conclusions of this study. The efficiency of excitation (or blowing) was always assessed in terms of C_μ, not the power consumption of the excitation device, because the latter was not optimized for this purpose.

A. Leading-Edge Excitation

Aerodynamic coefficients for lift, moment, and form drag, illustrating the effect of leading-edge blowing and excitation, are presented in Figs. 2a–2c, respectively, where solid lines indicate the upstroke and broken lines indicate the downstroke. Typical lift hysteresis, with stall occurring at maximum incidence, is evident for the baseline case (Fig. 2a) and the negative impact of blowing is manifested by the greatly magnified hysteresis loop, with $C_{L,\min} \approx 0.3$. In contrast to this, excitation at the same C_μ maintains a virtually identical up- and downstroke with a marginal increase in $C_{L,\max}$ and effectively eliminates lift hysteresis. These effects are emphasized by the moment coefficient data in Fig. 2b, where the baseline excursion is one and one-half times the allowable limit E_A, which is typical of light stall with $C_{M,\max} - C_{M,\min} \sim 0.1$. In the case of blowing, moment stall commences at approximately 15 deg and undergoes an excursion that is more than three times the allowable limit. In contrast, excitation delays moment stall and reduces the negative moment, resulting in acceptable excursions. The form-drag data Fig 2c illustrates, as expected, that blowing has an extremely detrimental effect, with drag stall commencing at approximately 13 deg, although excitation at this reduced frequency has a relatively small effect.

A summary of important aerodynamic indicators, across the range of effective F^+ and C_μ is presented in Figs. 3a–3c.[34] Figure 3a shows that the maximum lift attained by steady blowing for $C_\mu < 2\%$ is never significantly greater, and sometimes less, than the baseline case. More important, none of these data, including the baseline data, are considered valid because the moment excursions are never within the allowable limit (Fig. 2b). For $C_\mu > 3\%$, steady blowing brings about dramatic improvements in $C_{L,\max}$ and $C_{Dp,\mathrm{mean}}$ (Fig. 3c) while concomitantly the moment excursions are brought under control. This observation bears qualitative similarities to the flow visualization data of McAlister (see Ref. 1). Contrary to the earlier

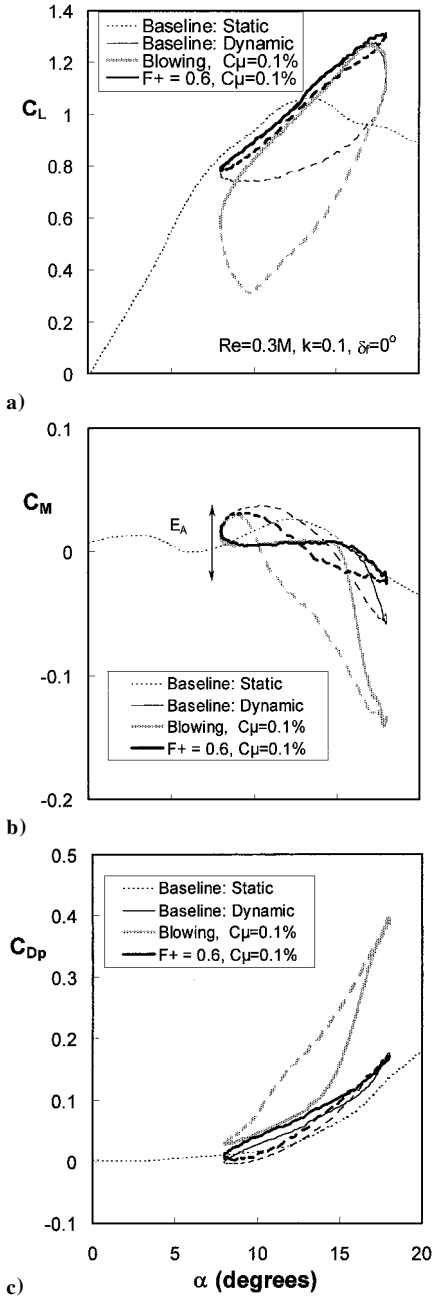

Fig. 2 Comparison of important aerodynamic coefficients for leading-edge blowing and excitation.

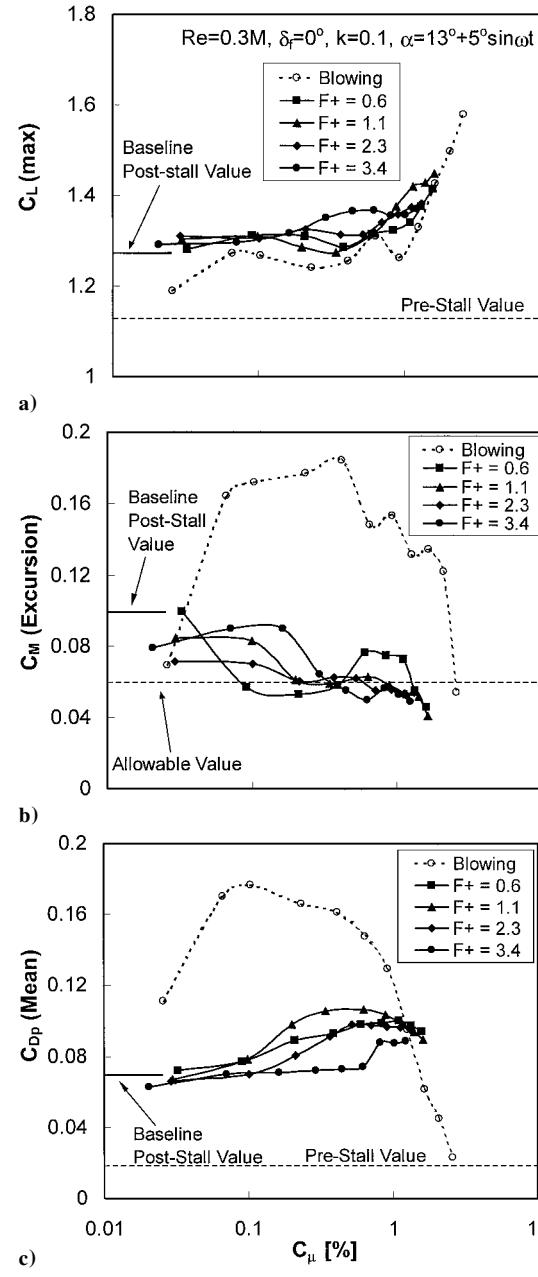

Fig. 3 Effect of excitation frequency and momentum coefficient on leading-edge blowing and excitation.

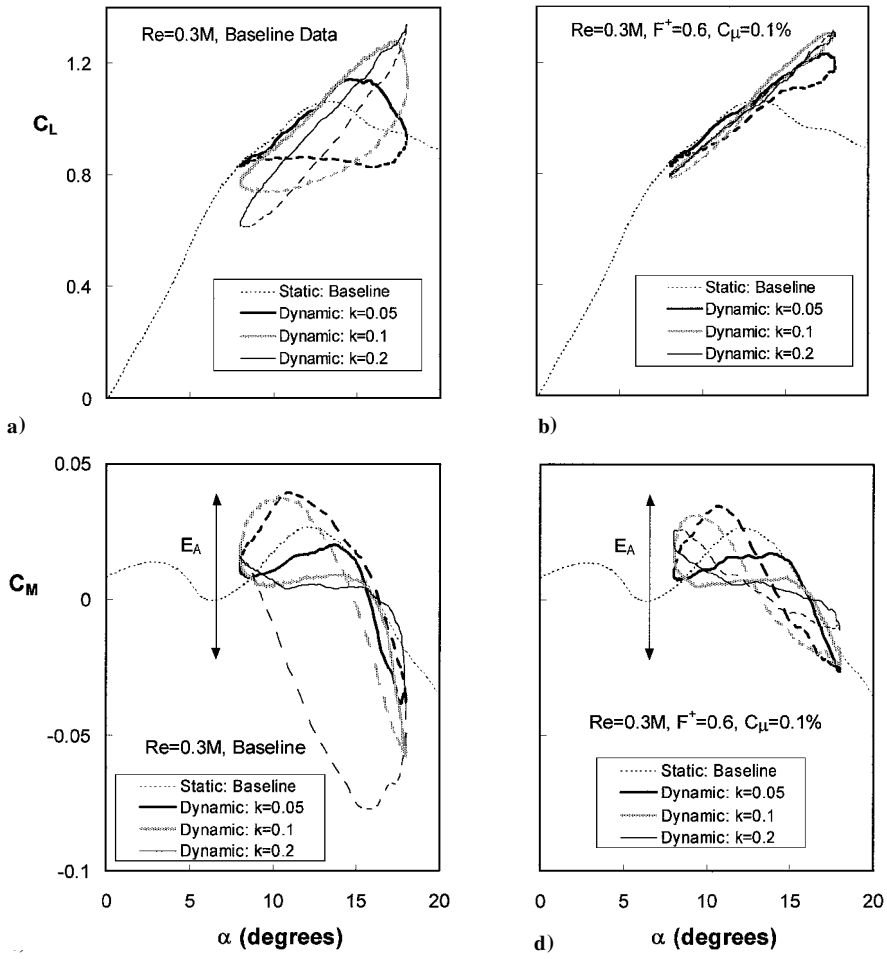

Fig. 4 Effect of airfoil oscillation rate on lift and moment for leading-edge excitation.

discussion, for excitation, $C_{L,\max}$ data are always greater than or equal to baseline data for $C_\mu > 0.1\%$ and corresponding moment excursions are within allowable limits. For $F^+ = 0.6$ with $C_\mu = 0.1\%$ (see Fig. 2) $C_{L,\max}$ increased by 16% over the prestall value with $\Delta C_{L,\max}/C_\mu = 160$. However, no single reduced frequency is capable of containing moment excursions for the entire C_μ range considered. Moreover, for a given C_μ, different reduced frequencies produce maximum lift. For example, $F^+ = 3.6$ produces the highest lift for $C_\mu \sim 0.5\%$, whereas $F^+ = 1.1$ is superior at higher C_μ. The mean form-drag data (Fig. 3c) indicate that excitation at all reduced frequencies is far superior to blowing at $C_\mu < 1\%$, but there are small increases in form drag with increasing momentum input, which attenuate with increasing F^+.

The effect of airfoil reduced frequency, $k = 0.05$, 0.1, and 0.2, on C_L and C_M, for baseline and leading-edge excitation ($F^+ = 0.6$ and $C_\mu = 0.1\%$ for all cases) is considered in Figs. 4a–4d. It is well known that dynamic stall data such as lift hysteresis, $C_{L,\max}$, and $C_{M,\text{exc}}$ are affected by the airfoil oscillation rate.[1] This dependence is demonstrated in Figs. 4a and 4c, which indicate that a larger $C_{L,\max}$ is obtained at higher k, but at the expense of larger moment excursions. Also, baseline lift hysteresis loops decrease with increasing k, whereas the opposite is true for baseline moment hysteresis loops. When excitation is applied, this dependence is almost completely eliminated (Fig. 4b), apart from a slight increase in $C_{L,\max}$ at higher k. Although baseline moment excursions E_A increase with increasing k, precisely the opposite is true when employing excitation because the excursions decrease with increasing k. For $k = 0.2$, the excursions are approximately one-third of the baseline value.

The effect of varying the mean incidence angle from 5 to 17 deg on lift and moment is shown in Figs. 5a–5d, for baseline and excitation ($F^+ = 3.6$ and $C_\mu = 0.4\%$) cases, respectively. As in static studies, excitation has very little effect on lift in the prestall regime, whereas the moment excursions are slightly attenuated. As the airfoil pitches beyond the static-stall angle, however, excitation increases $C_{L,\max}$ and controls the moment excursions (cf. Fig. 3). For incidence angles significantly larger than the static stall angle ($\bar{\alpha} \geq 17$ deg), excitation increases lift but is less effective in controlling moment excursions. These deep-stall cases are discussed in Sec. IV.D and further elaborated on in the companion paper.[30]

B. Effect of Aft-Loading Employing Flap Deflection

Dynamic stall control employing flap-shoulder excitation is a new concept[27,28] and requires some elaboration (see Fig. 6). Figure 6 shows C_L vs α characteristics typical of flapped or aft-loaded (trailing-edge stalling) airfoils, where three distinct regions can be discerned: I prestall, II partial stall emanating from the trailing-edge region, and III post-leading-edge stall. In static airfoil studies, flap-shoulder excitation attaches the flow over the flap[22] and in so- doing increases $C_{L,\max}$, that is, $\Delta C_{L,\max} = C_{L,\max}$ (excitation) $- C_{L,\max}$ (baseline), without significantly affecting the static-stall angle, as shown in Fig. 6. Steady blowing achieves the same $C_{L,\max}$ with approximately five times the momentum input, but at lower incidence. For a dynamically pitching airfoil with excitation or blowing at the flap shoulder, dynamic flap stall is controlled and not traditional leading-edge dynamic stall. Therefore, the method of control is somewhat different as will be shown.

An example of this principle is presented in Fig. 7, for a symmetric airfoil ($\delta_f = 0$ deg), under static and dynamic conditions described by $Re = 0.3 \times 10^6$, $k = 0.1$, $\alpha = 11 + 5\sin(\omega t - 90)$ deg. For this case, region I extends to approximately $\alpha = 6$ deg, and as a consequence, excitation in the vicinity of $\alpha_{\min}$ has little effect on C_L. With increasing incidence, however, the effects of excitation become more pronounced for both static ($\Delta C_{L,\max} = 0.36$) and dynamic ($\Delta C_{L,\max} = 0.3$) lift data. In addition, the moment excursion

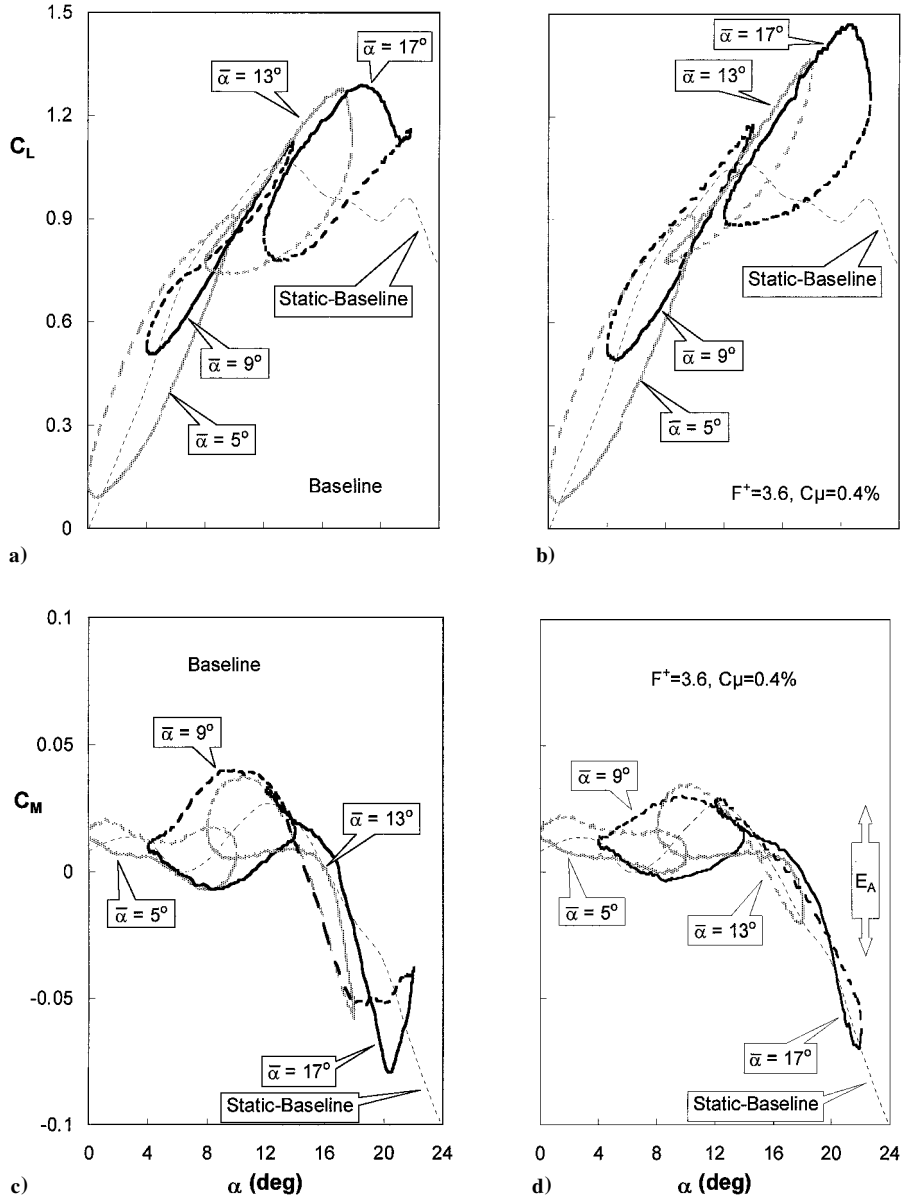

Fig. 5 Dynamic lift and moment data for a wide range of incidence angles, $Re = 3 \times 10^5$, and $k = 0.1$.

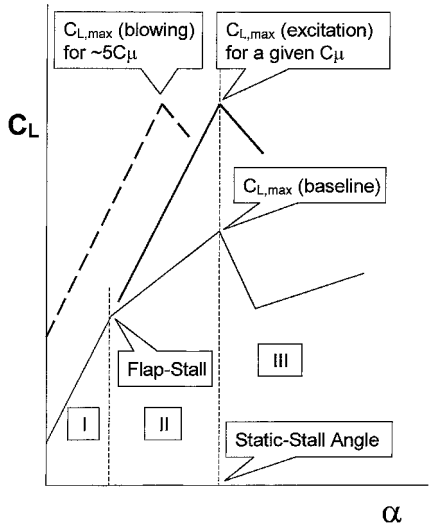

Fig. 6 Schematic of the means to attain dynamic flap-shoulder stall control by means of flap-shoulder excitation.

due to flap stall is reduced by a factor of three with excitation. Note that, in contrast to leading-edge excitation, flap-shoulder excitation increases $dC_L/d\alpha$ and, consequently, the C_L excursion (in addition to increasing $C_{L,\max}$), which is important for an advancing rotorcraft (see Sec. IV.C). Increasing the mean incidence angle by 1 deg brought about leading-edge stall in both cases, with resulting moment excursions larger than E_A (0.06).

The same strategy (Sec. III), as applied in the preceding section, was adopted for flap-shoulder excitation where $\delta_f = 20$ deg, $Re = 0.3 \times 10^6$, and static stall was at $\alpha_s = 12$ deg (2 deg less than the undeflected-flap case). The flap angle, as well as the excitation (F^+ and C_μ), was maintained constant throughout the oscillation cycle. The intention here was to emphasize the effect of airfoil aftloading in conjunction with oscillatory excitation. In an effort to obtain the largest $C_{L,\max}$ with C_M excursions bounded to within allowable excursions, as before, the mean incidence angle was increased to 10 deg. (Note that with $\delta_f = 20$ deg there is a nonzero mean nose-down pitching moment, $C_{M,\text{mean}} \sim 0.1$, but here we are concerned primarily with moment excursions.) Under these conditions $F^+ = 1.4$ was the most effective reduced frequency for $C_\mu < 1\%$ and was superior to steady blowing in this range.[31,35] At higher levels of flap-shoulder excitation (Fig. 8), $C_\mu > 1\%$,

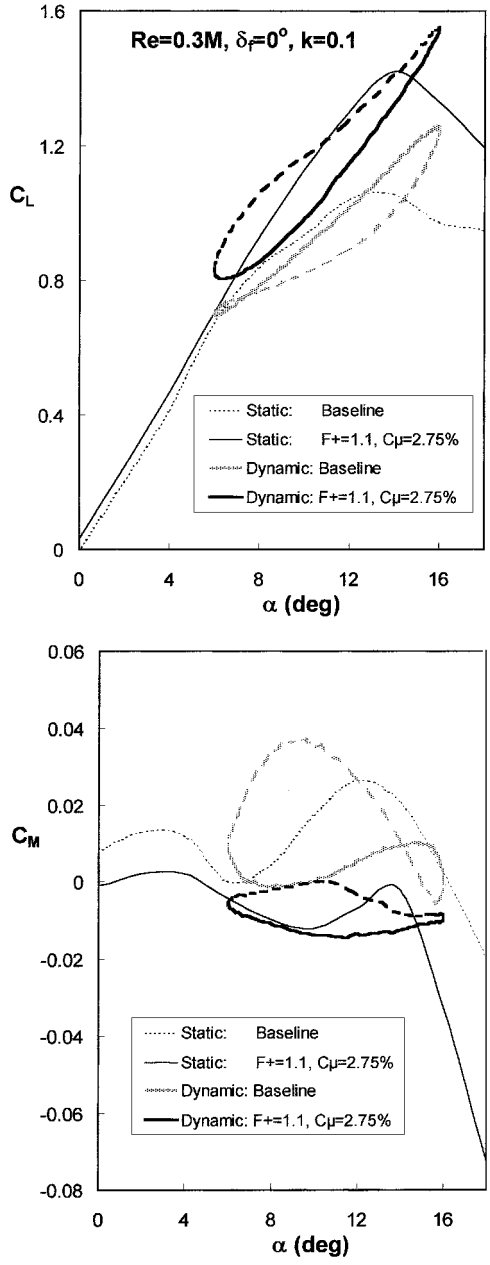

Fig. 7 Example of flap-shoulder excitation for the symmetric airfoil.

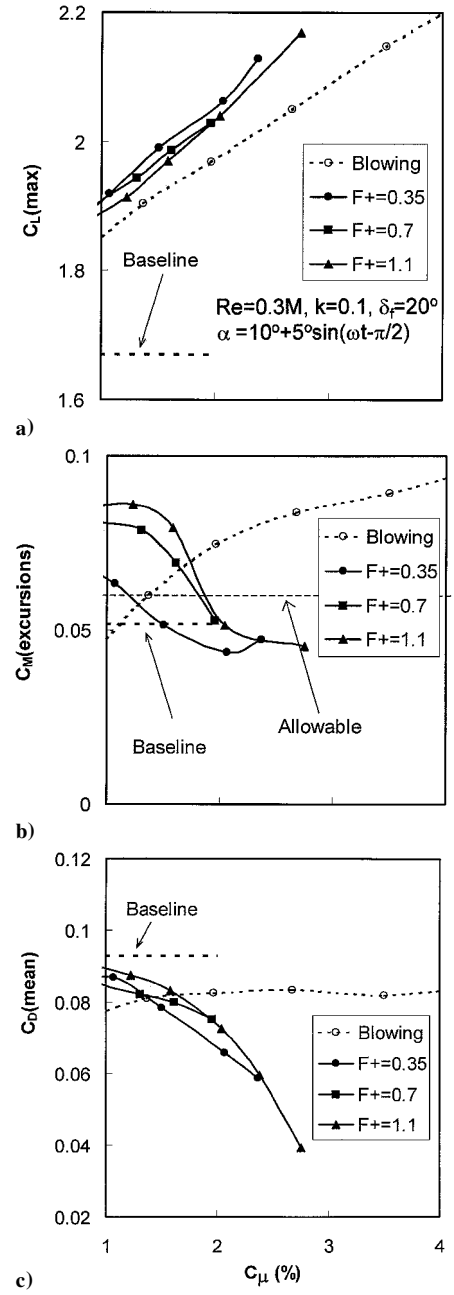

Fig. 8 Effect of flap-shoulder blowing and excitation on lift and drag for $C_\mu > 1\%$.

$F^+ = 0.35$ was the most effective reduced frequency, with regard to lift enhancement and moment excursion control, as well as overall mean drag reduction. The results for $F^+ = 0.7$ and 1.1 are also presented because they were effective at high C_μ; however, frequencies greater that $F^+ = 1.1$ were found to be less effective in containing moment excursions. Steady blowing increases lift proportionally to increase, in C_μ, but it was unable to attach the flap boundary layer as is evidenced by the steadily increasing moment excursions and the insensitivity of the mean drag to higher C_μ. Even when the steady C_μ was increased up to 15%, no significant mean drag reduction was observed.

The effect of steady blowing and oscillatory excitation on time mean total drag under the conditions described earlier, for $F^+ = 1.1$ and $C_\mu = 2.75\%$, is considered in Fig. 9 (cf. Fig. 8c). At low instantaneous α, blowing appeared to be effective at reducing drag, but as the airfoil pitched up, flap-shoulder blowing promoted leading-edge stall, in analogy to the static scenario (Fig. 6).[22,35] In contrast to this, excitation was effective in containing the momentum deficit throughout the oscillation cycle.[35] The time-mean data (Fig. 9) provides a quantitative representation of the earlier observations, where steady blowing results in a wake that is 25% wider than the baseline wake with a mean drag reduction of only 10%. For excitation at $F^+ = 1.1$, the lateral wake extent is reduced by 45% relative to the baseline value, with a 60% reduction in mean drag. Although, a large excitation amplitude was employed in the preceding example, the method remains effective with $\Delta C_{L,\max}/C_\mu = 20$ and $\Delta C_{D,\text{mean}}/C_\mu = 2$. For $C_\mu < 1\%$, differences between C_D and C_{Dp} were small, typically less than 10%. However, when employing excitation for $C_\mu > 2\%$, C_D was as much as 50% less than C_{Dp}.

The effect of the airfoil oscillation frequency k on C_L and C_M was assessed for the range $0.05 \le k \le 0.3$ and $\bar{\alpha} = 10$ deg with blowing and excitation.[31,35] Excitation was able to contain moment excursions throughout the range of airfoil oscillation frequencies, whereas blowing was as effective in this regard only for $k \ge 0.1$. With respect to $C_{L,\max}$, excitation was superior throughout the range of k, whereas blowing was inferior and totally ineffective for $k \ge 0.2$.

Previous studies on a generic flap[21] as well as on static airfoils[22] indicated that the range of reduced frequencies $2 < F^+ < 4$ were effective for separation delay, but this was not the case under the conditions mentioned earlier. Consequently, the mean incidence angle was

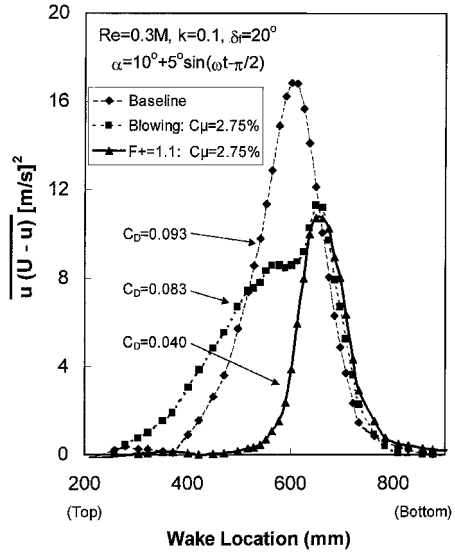

Fig. 9 Time-mean wake momentum deficit for flap-shoulder blowing and excitation.

lowered to $\bar{\alpha} = 7$ deg, such that the maximum incidence angle coincided with the static-stall angle (with $\delta_f = 20$ deg and $\alpha_S = 12$ deg). At this angle reduced frequencies $F^+ = 1.4$ and 2.5 were effective at increasing lift and reducing form drag, with the latter more effective in reducing mean form drag by 40% at $C_\mu = 0.6\%$. Consequently, airfoil efficiency, based on the quantity, $L_{\max}/D_{\text{mean}}$, was up to three times larger for $\bar{\alpha} = 7$ deg relative to $\bar{\alpha} = 10$ deg (Refs. 31 and 35). As before, excitation was far superior to blowing, particularly with regard to drag reduction.

C. Effect of Excitation Location

A question of considerable importance was how flap-shoulder excitation and leading-edge excitation compared for $\delta_f = 0$ deg, that is, a symmetric airfoil. Intuitively, and on the basis of all conventional attempts to control dynamic stall, control from the leading-edge region is the obvious choice. The results presented in Figs. 10a–10c, however, for excitation data ($F^+ = 1.1$, $C_\mu = 0.2\%$) with $C_{L,\max}$ equal in both cases (Fig. 10a) indicate precisely the opposite. This specific case was selected arbitrarily because the basic trends are the same for almost all (see next paragraph) C_μ and F^+ combinations. Flap-shoulder excitation produces larger C_L excursions, which ultimately determine the performance of an advancing rotorcraft as mentioned in Sec. IV.B. Figure 10b shows that both methods of excitation are able to contain the moment excursions, with the flap-shoulder excitation case yielding better results for the prescribed C_μ input. Figure 10c shows significant form-drag reductions with excitation emanating from the flap, whereas leading-edge excitation tends to increase form drag (see Sec. IV.A). Note that increasing $\bar{\alpha}$ did not affect $C_{L,\max}$ for leading-edge excitation, but only served to increase form drag. For flap-shoulder excitation, increases in $\bar{\alpha}$ increased $C_{L,\max}$, but moment excursions exceeded the allowable bounds.

An overall comparison for the $\delta_f = 0$ deg case is presented in Figs. 11a and 11b, which contain a comparison of $C_{L,\max}$, $C_{L,\text{exc}}$, and $C_{Dp,\text{mean}}$ for leading-edge and flap-shoulder excitation across the F^+ and C_μ range, where only the data that fall within acceptable moment-excursion limits are plotted. From Fig. 11a, the following is immediately obvious: On the whole, flap-shoulder excitation is more effective for increasing lift excursions in spite of a symmetric airfoil being employed. This finding contradicts much of the conventional wisdom associated with controlling dynamic stall. Note, however, that control is not exerted directly over the DSV, but rather over the separated trailing-edge region. As indicated previously,[28,31] leading-edge excitation is more erratic because moment excursions depend on both F^+ and C_μ. This is visible by the number of isolated data points for leading-edge excitation data. Additionally, leading-edge excitation is less effective at low C_μ because lift does not always increase with momentum input but, depending on the frequency, it exhibits local maxima (cf. Fig. 3). On the other hand, in the case of flap-shoulder excitation, variations in lift excursions are approximately monotonic with C_μ. A mean form-drag comparison (Fig. 11b) shows that flap-shoulder excitation reduces form drag much more effectively than leading-edge excitation, typically by a factor of 3.

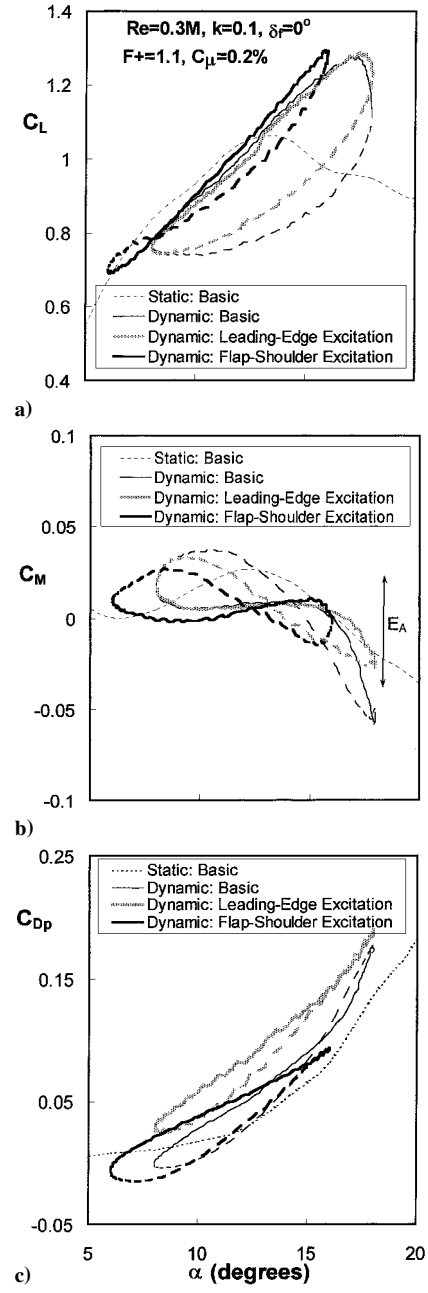

Fig. 10 Comparison of aerodynamic coefficients for leading-edge and flap-shoulder excitation for the symmetric airfoil.

When repeating similar comparison with increased simulated aft loading, that is, $\delta_f = 10$ and 20 deg (Ref. 31), three additional features are apparent: First, $C_{L,\max}$ is significantly larger for the flap-shoulder excitation case without exception; second, the difference in $C_{L,\max}$ increases with increasing C_μ; and third, the form drag begins to decrease significantly at $C_\mu > 1\%$ for flap-shoulder excitation.

D. Control of Deep Stall

Consider the aerodynamic coefficients when the mean incidence angle is increased to 20 deg such that $\alpha = 20 + 5\sin(\omega t - 90)$ deg,

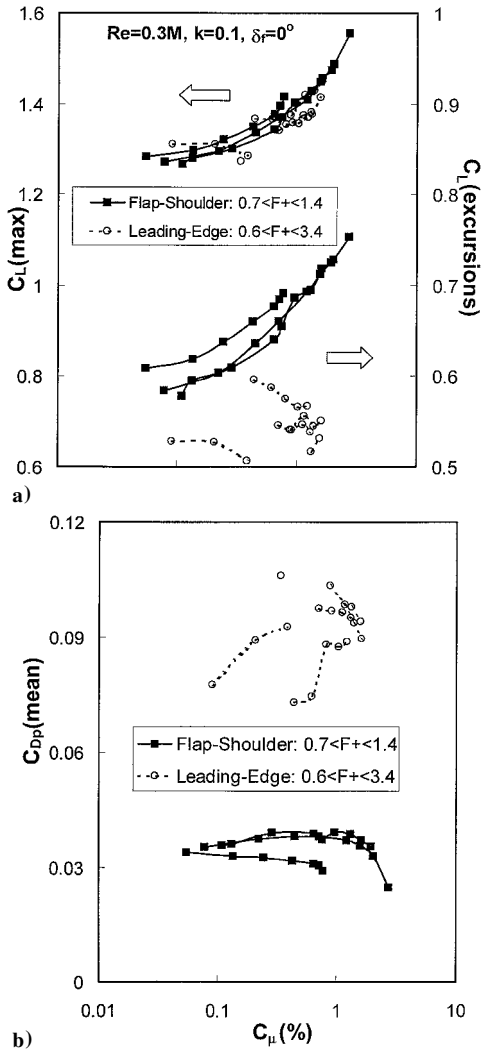

Fig. 11 Overall comparison of maximum lift and mean form drag for leading-edge and flap-shoulder excitation for the symmetric airfoil; only data with allowable moment excursions ($E_A \leq 0.06$) are plotted.

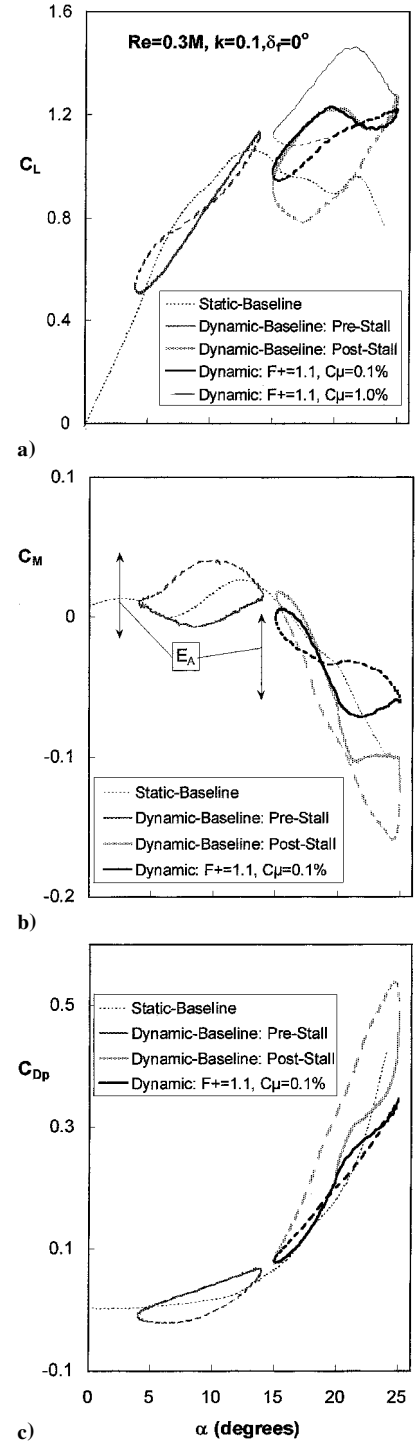

Fig. 12 Effect of leading-edge excitation on aerodynamic coefficients for low and high C_μ during deep stall.

$k = 0.1$, $Re = 0.3 \times 10^6$, and $\delta_f = 0$ deg (symmetric airfoil), as presented in Figs. 12a–12c. For this scenario, $\alpha_{\min}$ is a full degree above the static-stall angle. The baseline case shows relatively large hysteresis loops associated with lift, moment, and form drag, although the lift hysteresis loop looks peculiar, with the appearance of dynamic stall around $\alpha = 20$ deg followed by a lift increase between $\alpha = 24$ and 25 deg. This nonclassical dynamic stall was attributed to partial separation downstream of the leading edge, although at these large incidence angles wind-tunnel blockage may have been a factor. However, the additional lift at the end of the pitchup motion, caused by the dynamic stall vortex, bears qualitative similarity to published data.[1] During poststall, the large hysteresis loop bottoms out at $C_{L,\min} = 0.78$ when $\alpha = 17$ deg.

Figure 12 shows the effect of low ($C_\mu = 0.1\%$) and high ($C_\mu = 1\%$) excitation amplitudes at $F^+ = 1.1$. For $C_\mu = 0.1\%$, excitation at this reduced frequency had no effect on lift during the pitchup motion, apart from the region around $\alpha \approx 25$ deg, but significantly reduced the hysteresis during the downstroke phase with $C_{L,\min} = 0.95$ corresponding to $\alpha = 15$ deg. The moment excursion was significantly affected, where the trailing-edge separation was attenuated, but more important, leading-edge stall (or the leading-edge vortex) was effectively eliminated. The impact on mean form drag was a reduction of 36%. These lift and moment data bear qualitative resemblance to slat data,[1] where the $C_{L,\max}$ increase at the end of the pitchup phase (manifestation of the DSV) is attenuated and the moment excursion is significantly reduced. Increasing C_μ by an order of magnitude had a pronounced effect on lift, increasing $C_{L,\max}$ to 1.5 at $\alpha = 22$ deg and resulting in a more familiar hysteresis loop. The C_μ increase had a minimal effect on moment and form-drag histories, and thus, these data are not presented here. Airfoil performance, for a range of F^+, C_μ, and k was considered with similar results to those observed for light stall (see Sec. IV.A).[30] Time-mean total drag was a minimum at $F^+ = 2.5$, as in the case of flap-shoulder excitation, with a 25% reduction over the baseline case.[31] The shape of the wake profiles, however, was not as dramatically altered. More details on the mechanisms associated with the deep-stall control are presented in the companion paper.[30] As in the light-stall case, excitation at $F^+ = 0.6$ produced

the highest lift at $C_\mu = 0.1\%$, and the deep-stall data were shown to be independent of Reynolds number.[31]

V. Conclusions

The conducted parametric study yielded the following principle conclusions.

1) Light stall, as well as deep stall, were effectively controlled by oscillatory excitation.

2) The beneficial effects of excitation were more pronounced at higher airfoil oscillation rates and effectively independent of Reynolds number.

3) Flap-shoulder steady blowing was detrimental for $1\% \leq C_\mu \leq 15\%$, as was leading-edge blowing for $C_\mu < 1\%$.

4) For aft-loaded airfoils, flap-shoulder excitation was found to be superior to leading-edge excitation because a) higher overall $C_{L,\max}$ and/or $C_{L,\text{exc}}$ were achieved for the same C_μ, b) differences in $C_{L,\max}$ became more pronounced with increased airfoil aft loading, and c) flap-shoulder excitation was more effective at reducing mean drag for a given $C_{L,\max}$.

5) Flap-shoulder excitation, in conjunction with prestall pitch excursions, was more aerodynamically efficient than excitation employed in the poststall regime.

The current experimental program has been extended to include a more appropriate rotorcraft airfoil, that is, the NACA 0012, to attain a more realistic simulation of typical rotor-blade stall and its control. The profile has no flap and includes a slot at 5% chord, which does not affect the basic airfoil geometry. The profile chord is almost half that of the NACA 0015 used in this study to eliminate uncertainty caused by wind-tunnel blockage. Provisional static and dynamic data on the NACA 0012 confirm the main conclusions presented in this paper.[31]

To date, the effect of compressibility on dynamic stall control by excitation has not yet been assessed. Because dynamic stall is usually associated with the high-speed flow regime, assessment of compressibility effects should be a future research priority.

Acknowledgments

This work was sponsored in part by a Grant from the Research and Development Office of the Israel Ministry of Defense, monitored by A. Kuritzki, and is an assigned task of the U.S./Israel MOA on rotorcraft aeromechanics. Assistance from the Tel Aviv University Aerolab staff and graduate students is gratefully acknowledged.

References

[1]Carr, L. W., "Progress in the Analysis and Prediction of Dynamic Stall," *Journal of Aircraft*, Vol. 25, No. 1, 1988, pp. 6–17.

[2]McCroskey, W. J., "Unsteady Airfoils," *Annual Review of Fluid Mechanics*, Vol. 14, 1982, pp. 285–311.

[3]Stepniewski, W. Z., and Keys, C. N., *Rotary-Wing Aerodynamics*, Dover, New York, 1984.

[4]McCloud, K. L., III, Hall, L. P., and Brady, J. A., "Full-Scale Wind Tunnel Tests of Blowing Boundary Layer Control Applied to Helicopter Rotor," NASA TN D-335, 1960.

[5]Alrefai, M., and Acharya, M., "Controlled Leading-Edge Suction for Management of Unsteady Separation over Pitching Airfoils," *AIAA Journal*, Vol. 34, No. 11, 1996, pp. 2327–2336.

[6]Karim, M. A., and Acharya, M., "Suppression of Dynamic-Stall Vortices over Pitching Airfoils by Leading-Edge Suction," *AIAA Journal*, Vol. 32, No. 8, 1994, pp. 1647–1655.

[7]Luttges, M. W., Robinson, M. C., and Kennedy, D. A., "Control of Unsteady Separated Flow Structures on Airfoils," AIAA Paper 85-0531, March 1985.

[8]Weaver, D., McAlister, K. W., and Tso, J., "Suppression of Dynamic Stall by Steady and Pulsed Upper-Surface Blowing," AIAA Paper 98-2413, June 1998.

[9]Green, R. B., and Gilbraith, R. A. M., "An Investigation of Dynamic Stall Through the Application of Leading Edge Roughness," *18th European Rotorcraft Forum*, Paper 137, 1992.

[10]Wilder, M. C., Chandrasekhara, M. S., and Carr, L. W., "Transition Effects on Compressible Dynamic Stall of Transiently Pitching Airfoils," AIAA Paper 93-2978, July 1993.

[11]Chandrasekhara, M. S., Wilder, M. C., and Carr, L. W., "Boundary Layer Tripping Studies of Compressible Dynamic Stall Flow," AIAA Paper 94-2340, June 1994.

[12]Carr, L. W., Chandrasekhara, M. S., Wilder, M. C., and Noonan, K. W., "The Effect of Compressibility on Suppression of Dynamic Stalls Using a Slotted Airfoil," AIAA Paper 98-0332, Jan. 1998.

[13]Carr, L. W., and McAlister, K. W., "The Effect of a Leading-Edge Slat on the Dynamic Stall of an Oscillating Airfoil," AIAA Paper 83-2533, Oct. 1983.

[14]Yu, Y. H., Lee, S., McAlister, K. W., Tung, C., and Wang, C., "Dynamic Stall Control for Advanced Rotorcraft Application," *AIAA Journal*, Vol. 33, No. 2, 1995, pp. 289–295.

[15]Freymuth, P., Jackson, S., and Bank, W., "Toward Dynamic Separation Without Dynamic Stall," *Experiments in Fluids*, Vol. 7, 1989, pp. 187–196.

[16]Chandrasekhara, M. S., Wilder, M. C., and Carr, L. W., "Unsteady Stall Control Using Dynamically Deforming Airfoils," *AIAA Journal*, Vol. 36, No. 10, 1998, pp. 1792–1800.

[17]Hassan, A. A., "Numerical Simulations and Potential Applications of Zero-Mass Jets for Enhanced Rotorcraft Aerodynamic Performance," AIAA Paper 98-0211, Jan. 1998.

[18]Katz, Y., Nishri, B., and Wygnanski, I., "The Delay of Turbulent Boundary Layer Separation by Oscillatory Active Control," AIAA Paper 89-0975, March 1989.

[19]Katz, Y., Nishri, B., and Wygnanski, I., "The Delay of Turbulent Boundary Layer Separation by Oscillatory Active Control," *Physics of Fluids 1*, 1989, pp. 179–181.

[20]Nishri, B., "On the Dominant Mechanisms Governing Active Control of Separation," Ph.D. Dissertation, Dept. of Fluid Mechanics and Heat Transfer, Faculty of Engineering, Tel Aviv Univ., Ramat Aviv, Israel, Dec. 1995 (in Hebrew).

[21]Nishri, B., and Wygnanski, I., "Effects of Periodic Excitation on Turbulent Separation from a Flap," *AIAA Journal*, Vol. 36, No. 4, 1998, pp. 547–556.

[22]Seifert, A., Darabi, A., and Wygnanski, I., "Delay of Airfoil Stall by Periodic Excitation," *Journal of Aircraft*, Vol. 33, No. 4, 1996, pp. 691–698.

[23]Seifert, A., Bachar, T., Koss, T., Shepshelovich, M., and Wygnanski, I., "Oscillatory Blowing, a Tool to Delay Boundary Layer Separation," *AIAA Journal*, Vol. 31, No. 11, 1993, pp. 2052–2060.

[24]Naveh, T., Seifert, A., Tumin, A., and Wygnanski, I., "Sweep Effect on Parameters Governing Control of Separation by Periodic Excitation," *AIAA Journal*, Vol. 35, No. 3, 1998, pp. 510–512.

[25]Seifert, A., and Pack, L. G., "Oscillatory Control of Shock-Induced Separation," *Journal of Aircraft*, Vol. 38, No. 3, 2001, pp. 464–472, (Part of AIAA Paper 99-0925).

[26]Seifert, A., and Pack, L. G., "Oscillatory Control of Separation at High Reynolds Numbers," *AIAA Journal*, Vol. 37, No. 9, Sept. 1999, pp. 1063–1071, (Part of AIAA Paper 98-0214).

[27]Greenblatt, D., Seifert, A., and Wygnanski, I., "Dynamic Stall Management by Oscillatory Forcing," *Euromech Colloquium 361: Active Control of Turbulent Shear Flows*, Technische Universität, Berlin, 1997.

[28]Greenblatt, D., and Wygnanski, I., "Dynamic Stall Control by Oscillatory Forcing," AIAA Paper 98-0676, Jan. 1998.

[29]Greenblatt, D., Darabi, A., Nishri, B., and Wygnanski, I., "Separation Control by Periodic Addition of Momentum with Particular Emphasis on Dynamic Stall," American Helicopter Society, Paper T3-4, April 1998.

[30]Greenblatt, D., Nishri, B., Darabi, A., and Wygnanski, I., "Dynamic Stall Control by Periodic Excitation, Part 2: Mechanisms," *Journal of Aircraft*, Vol. 38, No. 3, 2001, pp. 439–447.

[31]Greenblatt, D., "Dynamic Stall Control by Oscillatory Excitation," Ph.D. Dissertation, Dept. of Fluid Mechanics and Heat Transfer, Faculty of Engineering, Tel Aviv Univ., Ramat Aviv, Israel, Nov. 1999.

[32]Piziali, R. A., "2-D and 3-D Oscillating Wing Aerodynamics for a Range of Angles of Attack Including Stall," NASA TM 4632, 1994.

[33]Donovan, J. F., Kral, L. D., and Cary A. W., "Active Flow Control Applied to an Airfoil," AIAA Paper 98-0210, Jan. 1998.

[34]Greenblatt, D., Darabi, A., Nishri, B., and Wygnanski, I., "Some Factors Affecting Stall Control with Particular Emphasis on Dynamic Stall," AIAA Paper 99-3504, June–July 1999.

[35]Greenblatt, D., and Wygnanski, I., "Parameters Affecting Dynamic Stall Control by Oscillatory Excitation," AIAA Paper 99-3121, June–July 1999.

[36]McCroskey, W. J., McAlister, K. W., Carr, L. W., and Pucci, S. L., "An Experimental Study of Dynamic Stall on Advanced Airfoil Sections," NASA TM-84254, July 1982.

[37]Brinkworth, B. J., *An Introduction to Experimentation*, 2nd ed, English Universities Press, 1973.